Mem. S.A.It. Vol. 74, 683

Memorie della

Wave dissipation in Coronal Force-Free Structures

F. Malara[1,2], M. F. De Franceschis[1,2], and P. Veltri[1,2,]

[1] Dipartimento di Fisica, Università della Calabria, via P. Bucci, 87036 Rende (CS), Italy e-mail: malara@fis.unical.it
[2] Istituto Nazionale per la Fisica della Materia, Unità di Cosenza, via P. Bucci, 87036 Rende, Italy

Abstract. The dissipation of Alfvénic perturbations in a 3D magnetic equilibrium is studied. Assuming a plasma $\beta \ll 1$ a force-free magnetic field is calculated, which models the coronal field in a quiet sun region. The field has a complex structure due to the presence of several components at different spatial scales. The time evolution of Alfvénic wavepackets is calculated in the WKB approximation for a cold plasma. We find that the packet wavevector exponentially increases, due to the topological complexity of the equilibrium field, resulting in a fast dissipation of the wave energy. The dissipation time is proportional to the logarithm of the Reynolds number, as already found in similar contexts. The results are relevant for the coronal heating problem.

Key words. Coronal heating – Alfvén waves – Force-free magnetic field

1. Introduction

Coronal heating represents one of the most studied problems within solar physics. Dissipation of Alfvén waves is one of the mechanisms proposed to explain the high temperature observed in the solar Corona. These waves, which are directly observed in the solar wind, are probably generated by photospheric motions and are able to propagate through the strong gradients of the transition region.

Due to the very low values of relevant dissipation coefficients, the main theoretical problem is how to efficiently dissipate waves, before they leave the Corona. The presence of transverse gradients could help dissipation, since small scales are created in the wave pattern (see, e.g., Malara & Velli (1994) for a review). Typical mechanisms are either resonant absorption or phase mixing. The latter is very efficient in a 3D-structured magnetic fields where chaotic field lines are present; in this case, small scale generation proceeds exponentially in time, and the dissipation time scales as $t_d \propto \log S$, with S the relevant Reynolds and/or the Lundquist number (Similon & Sudan 1989; Petkaki et al. 1998). Such mechanism has been studied by Malara et al. (2000) for some force-free magnetic equilibria. In this paper we improve such study in two aspects: (i) we will

Send offprint requests to: F. Malara
Correspondence to: Dipart. di Fisica, via P. Bucci, 87036 Rende (CS), Italy

consider Alfvén wave propagation in a cold plasma; this is closer to the low-β coronal plasma, with respect to the incompressible plasma considered by Malara et al. (2000); (ii) the equilibrium magnetic field will be more realistic for the Corona.

2. The model

We consider Alfvénic perturbations propagating in a 3D magnetic field equilibrium structure. In Corona the gas pressure P_{gas} is much less than magnetic pressure $P_{magn} = B^2/8\pi$, so the plasma parameter $\beta = P_{gas}/P_{magn} \ll 1$. Thus, in our model compressibility is retained, but we assume $\beta = 0$ (cold plasma). In that case, the equilibrium magnetic field $\mathbf{B}$ must be a force-free field, i.e., it satisfies the equation

$$\nabla \times \mathbf{B} = \alpha \mathbf{B} \quad (1)$$

We use a planar geometry, in which the curvature is neglected; this is suitable to represent relatively small regions within the Corona. In the reference frame we used the xy plane represents the base of the Corona, while the z axis is in the vertical direction. We assume also statistical homogeneity in the horizontal directions; this is verified in quiet sun regions, where the photospheric magnetic field appears to be distributed at various spatial scales with no definite patterns. This is simulated by assuming periodicity along x and y directions, over a length $L \sim 10^4$-10^5 km. As a consequence, the magnetic field is expanded in Fourier series in the x and y variables In order to find a simple solution to equation (1), we assumed $\alpha = \text{const}$ (linear force-free field), requiring that B vanishes for $z \to +\infty$. Under the above assumptions Nakagawa & Raadu (1972) found a solution, which we re-write in the following form:

$$B_x(x,y,z) = \sum_k 2\frac{(k_x h - \alpha k_y)}{k^2} \times$$
$$a(k_x,k_y)\cos[\phi_{k_x,k_y}(x,y)]\exp(-hz) \quad (2)$$

$$B_y(x,y,z) = \sum_k 2\frac{(k_y h + \alpha k_x)}{k^2} \times$$
$$a(k_x,k_y)\cos[\phi_{k_x,k_y}(x,y)]\exp(-hz) \quad (3)$$

$$B_z(x,y,z) = -\sum_k 2a(k_x,k_y)$$
$$\sin[\phi_{k_x,k_y}(x,y)]\exp(-hz) \quad (4)$$

where

$$\sum_k = \sum_{\substack{k_x>0,k_y,\\ \alpha<k\le k_{max}}} + \sum_{\substack{k_x=0,k_y>0,\\ \alpha<k\le k_{max}}}$$

with $k_x = 2\pi n_x/L$ and $k_y = 2\pi n_y/L$ the horizontal wavevectors; n_x and n_y integers; $k = (k_x^2+k_y^2)^{1/2}$; $h = (k^2-\alpha^2)^{1/2}$; $\phi_{k_x,k_y}(x,y) = k_x x + k_y y + \varphi(k_x,k_y)$. The parameter α determines both the current associated with the magnetic field and the maximum length $l_{max} = 2\pi/\alpha$. In order to reproduce statistical homogeneity $l_{max} < L$ (Pommois et al. 1998); thus, we used $\alpha = 3.5(2\pi/L)$ and the phases $\varphi(k_x,k_y)$ have been randomly chosen in the interval $[0,2\pi]$. The maximum wavevector is $k_{max} = 6(2\pi/L)$, giving 38 Fourier components in the expressions (2)-(4). These components are originated by a turbulent cascade process taking place under the coronal base. Assuming a spectral energy density for the magnetic field $\epsilon(k) \propto k^{-5/3}$ we get $a(k_x,k_y) \propto k^{-4/3}$. Finally, we assumed a constant background density ρ, even though this assumption is not essential and it can be easily relaxed.

Alfvénic perturbations propagate in the above magnetic equilibrium. We assume that the wavelength is smaller than the typical length scale of the equilibrium field, which allows us to use the WKB approximation. Equations describing the evolution of both Alfvén and magnetosonic waves are then obtained. Considering Alfvén perturbations, these are decomposed as a superposition of localized wavepackets. Then, the following equations are obtained (a detailed derivation is given in Malara et al. (2003)):

$$\frac{d\xi_j}{dt} = c_{Aj} \quad (5)$$

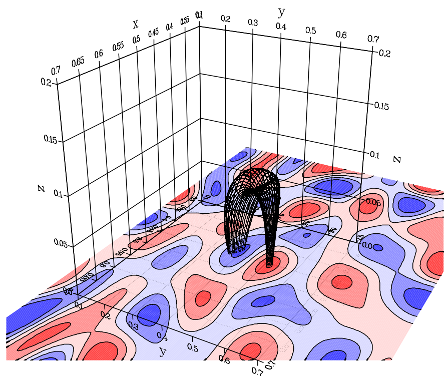

Fig. 1. Magnetic lines of a "compact" flux tube. Grey scale indicate the intensity of B_z at the coronal base.

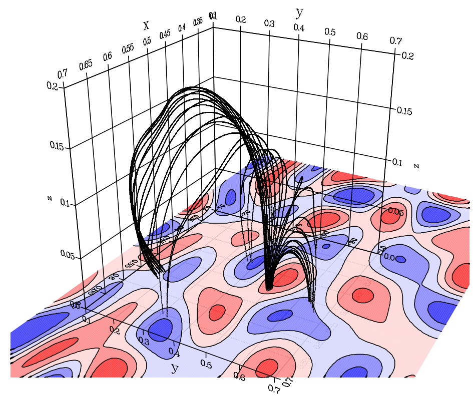

Fig. 2. Magnetic lines of a "broken" flux tube. Grey scale indicate the intensity of B_z at the coronal base.

$$\frac{d\kappa_j}{dt} = -\frac{\partial c_{An}}{\partial \tau} k_n \tag{6}$$

$$\frac{de}{dt} = -\frac{\kappa^2}{S} e \tag{7}$$

where ξ, κ, and e are the position, the wavevector, and the energy of the Alfvénic packet; $\mathbf{c_A} = \mathbf{B}/(\mathbf{4}\pi\rho)^{\mathbf{1/2}}$ is the Alfvén velocity, $\mathbf{B}$ and ρ the equilibrium magnetic field and density; S is the Reynolds/Lundquist number. The above quantities are dimensionless. The equations (5)-(7) have been numerically integrated, using for each packet the initial conditions $\xi_z = 0$, $\kappa_x = \kappa_y = \kappa_z = 20\pi$, $e = 1$, with ξ_x and ξ_y in the periodicity domain.

3. Results

Since the density is assumed to be constant, the trajectories of wavepackets obtained from equation (5) give also the lines of the equilibrium magnetic field $\mathbf{B}$. The topology of $\mathbf{B}$ is very complex. In order to illustrate it, we considered flux tubes, obtained by calculating the magnetic lines starting from a small circle located at the coronal base. Two different examples are shown in figures 1 and 2. The flux tube of figure 1 is "compact", i.e., the initial circle is mapped in a closed curve onto the coronal base. On the contrary, the flux tube of figure 2 is "broken", i.e., the magnetic surface separates into various sheets, which reach the coronal base at different locations, far away from one another. Those magnetic lines which are close to the separation points are "singular", since a small variation in the initial positions can move the line from one sheet to another, thus resulting in a totally different final position.

When a wavepacket propagates along a singular line, nearby lines diverge from it, thus resulting in a stretching of the packet. Correspondingly, the wavevector κ associated to the packet is strongly increased, and the dissipation rate is enhanced. Another mechanism of wavevector growth is related to the exponential dependence on the vertical z variable in the equilibrium magnetic field (see equations (2)-(4)): trajectories starting at the same time at the coronal base in nearby positions tend to move apart from one another exponentially in time. This results in an exponential growth of the wavevector κ. In figure 3 the wavevector κ is plotted as a function of time, for a given packet. It can be seen that the growth of κ is roughly exponential, and the final value is about 2 orders of magnitude larger than the initial value. In figure 4 the time evolution of the packet energy e is repre-

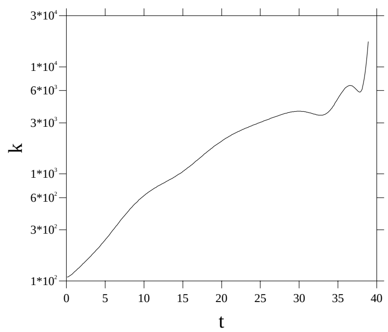

Fig. 3. The wavevector κ as a function of time t, for a given packet.

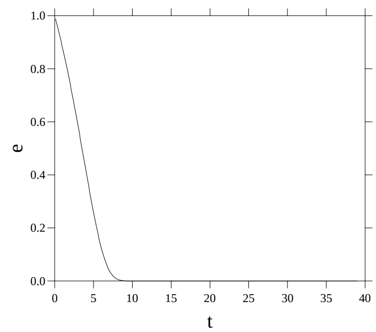

Fig. 4. The energy e as a function of time t, for a given packet, at $S = 10^5$

sented, for a value of the Reynolds number $S = 10^5$. It is seen that the initial energy is dissipated within few Alfvén times. The dissipation time t_d is defined by the relation $e(t_d)/e(0) = \exp(-1)$. A similar behavior has been observed for many other wavepackets, even though both the growth rate of κ and the dissipation time undergo large variations, according to the particular trajectory of the packet. The dissipation time increases with increasing the Reynolds number. In figure 5 t_d is plotted as a function of S for a given wavepacket. The scaling law $t_d \propto \log S$ is approximately verified for large S. This law, which is related to the exponential growth of κ, is the same as that found by Petkaki et al. (1998).

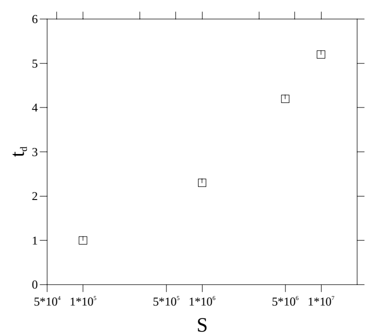

Fig. 5. The dissipation time t_d as a function of the Reynolds number S. A straight line corresponds to $t_d \propto \log S$.

Acknowledgements. This work has been performed in the framework of European Network "Theory, Observation and Simulation of Turbulence" and of the Center for High-Performance Computing (Centro di Eccellenza MIUR) of the University of Calabria. It has been supported by the Italian Ministero per l'Università e la Ricerca Scientifica (Cofin 2002).

References

Malara, F., & Velli, M. 1994, in Solar Coronal Structures, V. Rusin, P. Heinzel and J.-C. Vial eds., p. 443

Malara, F., Petkaki, P., & Veltri, P. 2000, ApJ 533, 523

Malara, F., De Franceschis, M. F., & Veltri, P. 2003, in preparation

Nakagawa, Y., & Raadu, M. A. 1972, Sol. Phys. 25, 127

Petkaki, P., Malara, F., & Veltri, P. 1998, ApJ 500, 483

Pommois, P., Zimbardo. G., & Veltri, P. 1998, Phys. Plasmas 5, 1288

Similon, P. L., & Sudan, R. N. 1989, ApJ 336, 442